Since January 2020 Elsevier has created a COVID-19 resource centre with free information in English and Mandarin on the novel coronavirus COVID-19. The COVID-19 resource centre is hosted on Elsevier Connect, the company's public news and information website.

Biosensors and Bioelectronics 223 (2023) 115037

Contents lists available at ScienceDirect

Biosensors and Bioelectronics

journal homepage: www.elsevier.com/locate/bios

Rapid quantitation of SARS-CoV-2 antibodies in clinical samples with an electrochemical sensor

Sanjay S. Timilsina [a,1], Nolan Durr [a,1], Pawan Jolly [a], Donald E. Ingber [a,b,c,*]

[a] Wyss Institute for Biologically Inspired Engineering, Harvard University, 02115, USA
[b] Vascular Biology Program, Boston Children's Hospital, And Harvard Medical School, 02115, USA
[c] Harvard John A. Paulson School of Engineering and Applied Sciences, Harvard University, 02115, USA

ARTICLE INFO

Keywords:
Electrochemical sensor
SARS-CoV-2 antibodies
Serology
Diagnostic
Dried blood spot

ABSTRACT

The current coronavirus disease 2019 (COVID-19) pandemic is caused by several variants of severe acute respiratory syndrome coronavirus-2 virus (SARS-CoV-2). With the roll-out of vaccines and development of new therapeutics that may be targeted to distinct viral molecules, there is a need to screen populations for viral antigen-specific SARS-CoV-2 antibodies. Here, we report a rapid, multiplexed, electrochemical (EC) device with on-chip control that enables detection of SARS-CoV-2 antibodies in less than 10 min using 1.5 μL of a patient sample. The EC biosensor demonstrated 100% sensitivity and specificity, and an area under the receiver operating characteristic curve of 1, when evaluated using 93 clinical samples, including plasma and dried blood spot samples from 54 SARS-CoV-2 positive and 39 negative patients. This EC biosensor platform enables simple, cost-effective, sensitive, and rapid detection of anti-SARS-CoV-2 antibodies in complex clinical samples, which is convenient for evaluating humoral-responses to vaccination or infection in population-wide testing, including applications in point-of-care settings. We also demonstrate the feasibility of using dried blood spot samples that can be collected locally and transported to distant clinical laboratories at ambient temperature for detection of anti-SARS-CoV-2 antibodies which may be utilized for serological surveillance and demonstrate the utility of remote sampling.

1. Introduction

The ongoing global pandemic due to infections with severe acute respiratory syndrome coronavirus-2 virus (SARS-CoV-2) has resulted in infection of millions of individuals as well as huge vaccination efforts on global scale to battle this highly infectious disease (Turgeon et al., 2021). Real-time reverse transcription polymerase chain reaction (RT-PCR) and rapid-antigen-detection are used to test for the presence of SARS-CoV-2 RNA and proteins in symptomatic and asymptomatic individuals (Abdelhamid and Badr, 2021; Mavrikou et al., 2020; Rasmi et al., 2021). While this was extremely critical at the start of pandemic, interest in serologic testing of blood has increased more recently because it can detect antibodies against specific viral proteins (Morales-Narváez and Dincer, 2020; Yakoh et al., 2021). This is important because this approach can be used to assess whether patients had prior COVID-19 infection and determine the efficacy, duration, and longevity of vaccine responses, as well as qualify convalescent plasma for therapeutic purposes (Najjar et al., 2022; West et al., 2021). Moreover, longitudinal evaluation of antibody titers in large populations is essential to evaluate the strength and extent of immunity generated by exposure to the virus, its variants, or the vaccines, and all this information is crucial for implementing effective public policy and vaccination strategies (Elledge et al., 2021; Jeyanathan et al., 2020; Seow et al., 2020).

Current COVID-19 vaccines induce the production of antibodies against the SARS-CoV-2 Spike (S) protein, but not against its nucleocapsid (N) protein. However, natural infection produces antibodies against both proteins, and thus diagnostic discrimination between these responses can help to differentiate natural immunity from vaccine-induced immunity (Gazit et al., 2021). Traditional serological assays are not optimal for assessing antibody levels under pandemic conditions as enzyme-linked immunosorbent assays (ELISAs) take several hours to complete due to the need for multiple incubation and washing steps (Sanjay et al. 2015, 2016, 2020). Lateral flow immunoassays (LFIAs) are more rapid, but they produce less reliable results and are qualitative

* Corresponding author. Wyss Institute at Harvard University, CLSB5, 3 Blackfan Circle, Boston, MA, 02115, USA.
E-mail address: don.ingber@wyss.harvard.edu (D.E. Ingber).
[1] Current address: StataDX Inc., Boston, MA 02215, USA.

https://doi.org/10.1016/j.bios.2022.115037
Received 12 November 2022; Received in revised form 16 December 2022; Accepted 22 December 2022
Available online 24 December 2022

rather than quantitative (Dou et al., 2015; Flower et al., 2020; Michel et al., 2020). Rapid antigen detection tests (RADTs) now widely used in the United States for detection of viral proteins could be adapted for detection of antibodies, but they have low sensitivity (Kanjilal et al. 2022a, 2022b). Another option would be use of chemiluminescent enzyme immunoassays (CLIAs) (Abbott and Roche Elecsys), however, they are costly, lack scalability, and need intricate analytical platforms (Tan et al., 2021). Many of these tests also must be carried out in a clinical research laboratory. Guidelines implemented to prevent spread of viral infections such as SARS-CoV-2 during serological surveillance also make collection of venous blood logistically difficult and have generated interest in dried blood spot (DBS) sampling. This is because the blood can be self-collected via a finger prick at-home or in community health centers and shipped to test sites at room temperatures (Wong et al., 2022). Through their ease of storage and shipment, low cost, and minimally invasive nature, DBSs can be employed to screen large populations for antibody titers even in low-resource settings. DBSs only require a few microliters of blood, can be easily multiplexed and automated, and are compatible with a range of bioanalytical methods, namely chromatography, spectroscopy, and immunoassays (Demirev, 2013). Also, refrigeration is not necessary for shipment and storage of DBS samples and results obtained with these samples have been shown to correlate well with those obtained from plasma or serum using ELISAs or commercial SARS-CoV-2 antigen and antibody assays (Amini et al., 2021; Zava and Zava, 2021). Proper packaging and shipment of DBS samples from home directly to a clinical laboratory for testing makes it a nonregulated material (Control and C.f.D., 2017; Zava and Zava, 2021). Thus, there is high demand for rapid and cost-effective detection approaches to monitor levels of different SARS-CoV-2 antibodies in order to assess patient responses to infections and vaccines in a timely manner (Cabrera et al., 2022; Kumar et al., 2022; Rahman, 2022). These biosensors with high sensitivity and specificity may be used either in low-resource settings or clinical laboratories in combination with use of DBS sampling.

Here, we report an electrochemical (EC) biosensor that enables ultrarapid, sensitive, and extremely specific detection of antibodies against SARS-CoV-2 from both plasma and DBS in minutes (Fig. 1). The biosensor is coated with a previously reported antifouling nanomaterial-based coating made of bovine serum albumin (BSA) and doped with highly conducting pentaamine-modified graphene nanoflakes (prGOx) that is cross linked with glutaraldehyde (GA). The nanomaterial-based coating efficiently prevents biofouling for at least 9 weeks and reduces non-specific binding thereby greatly increasing assay sensitivity, and has been fully characterized previously (Timilsina et al., 2022a). To generate a serologic assay with high sensitivity and specificity for SARS-CoV-2, specific ligands were covalently immobilized on the coated EC sensor to detect antibodies against specific viral proteins. The EC sensors can also be multiplexed to detect multiple different anti-virus antibodies simultaneously while also including on-chip controls. Analysis of plasma and DBS samples from 93 COVID-19 patients revealed that the EC sensor platform displayed 100% sensitivity and specificity with area under the ROC Curve (AUC) of 1. The assay can be performed in <10 min using only 1.5 μL of clinical sample.

2. Methods

2.1. Fabrication of electrochemical (EC) sensors

Gold-coated 4 plex sensor chips procured from Telic Company were cleaned using the protocol as reported earlier (Del Río et al., 2019). The anti-fouling nanomaterial-based coating was formulated either by using 5 mg/mL of BSA or Exbumin (Recombinant human albumin excipient, InVitria, CO, USA) in PBS with 8 mg/mL of prGOx. The resulting composite solution was mixed gently using a vortex mixer and sonicated for half an hour as reported earlier (Timilsina et al., 2022a). Thereafter coating was heat-denatured at 105 °C for 5 min and kept at 4 °C until further use. The excess black agglomerate of undissolved graphene was removed from the nanomaterial solution by centrifugation. Before adding the coating to the cleaned sensors, GA was added to the clear nanomaterial supernatant solution to crosslink the nanomaterial in 70:2 ratio (Timilsina et al., 2022a). Cleaned gold sensors were placed on a hot plate set to 85 °C for 2 min. After the sensors were equilibrated to 85 °C, 70 μL of nanomaterial coating was drop cast over each sensor for 45s (Timilsina et al. 2021, 2022b). Thereafter, sensors were immediately

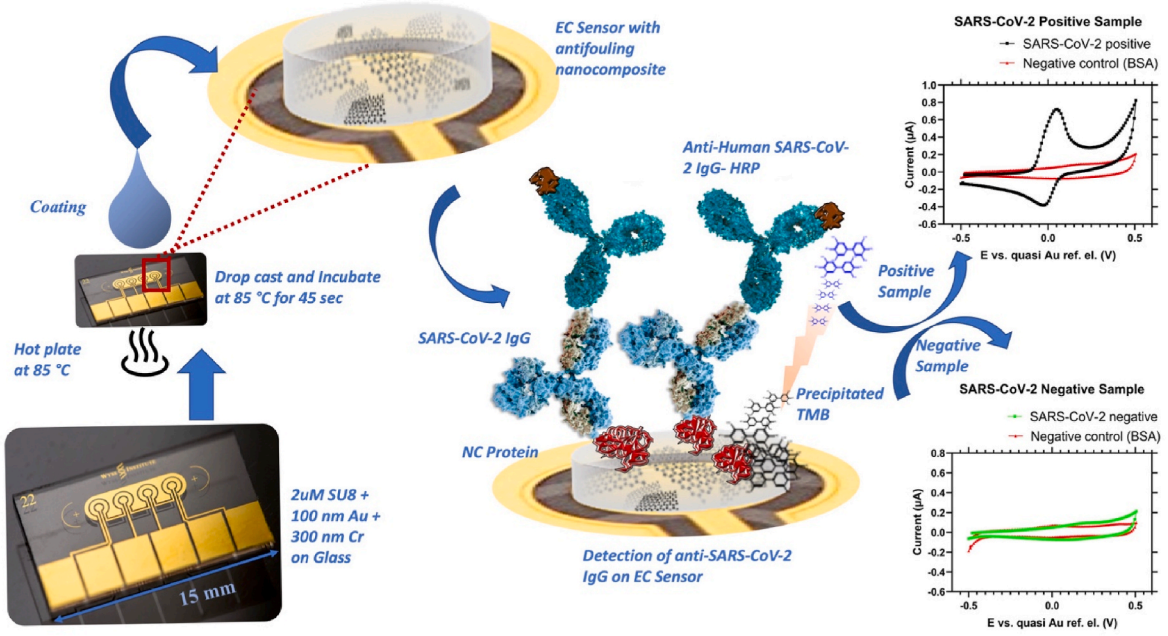

Fig. 1. Schematic of the multiplexed EC sensor platform. The antifouling nanocomposite is rapidly drop cast on the gold electrodes of the EC sensor (left). A sandwich assay was used to measure SARS-CoV-2 IgG bound to Nucleocapsid (NC Protein) that was pre-immobilized on the nanocomposite coating above sensor where TMB precipitates to generate an EC signal (middle). The top and bottom graphs represent CV for positive and negative SARS-CoV-2 samples, respectively, with on-chip negative control.

rinsed in PBS followed by drying for further use.

2.2. Detection of SARS-CoV-2 IgG in EC-biosensor and ELISA

Nanocomposite-coated sensors were activated using MES buffer (2 (N-morpholino) ethanesulfonic-acid) consisting of 400 mM of 1-ethyl-3 (3-dimethyl-aminopropyl)carbodiimide-hydrochloride (EDC) and 200 mM of N hydroxysuccinimide(NHS) to conjugate the capture protein as described previously (Najjar et al., 2022). The coated sensors were activated for half an hour at ambient temperature in the dark. Then the sensors were quickly washed with water (Milli-Q) and air-dried. Capture protein (0.6 mg/mL) was then spotted over the three gold-working-electrode areas with a capillary pin. BSA or rHA was spotted on the fourth gold-working-electrode as a negative control. The biosensors were kept overnight in a humid chamber at 4 °C. After bio-conjugation, sensors were rinsed with PBS to remove any unbound proteins followed by quenching of unreacted groups with 1 M-ethanolamine for half an hour. Finally, 2.5% BSA/rHA in PBS was used to block the sensors for an hour and stored until further use.

Positive and negative SARS-CoV-2 plasma samples were diluted 10-fold using 1% BSA/rHA in PBS. Mouse monoclonal anti-Human IgG Fc (abcam, no. ab99759) linked with HRP (horseradish peroxidase) was diluted to 40 μg/mL in 1% BSA/rHA in PBS. 18:2 ratio of diluted clinical samples and HRP-detection antibody were mixed and 15 μL was pipetted to each biosensor and incubated for 7 min. Wash buffer (PBST) was prepared by adding 0.05% Tween-20 to PBS. After rinsing with wash buffer, 10 μL of precipitating substrate 3,3′,5,5′ Tetramethyl-benzidine, (TMB, Sigma Aldrich, USA) was pipetted to biosensors for a min. After the final wash, precipitated signals from TMB were measured in 10 μL of PBST with a potentiostat (Autolab PGSTAT128N, Metrohm). Cyclic voltammetry was performed between the potential of 0.5 to −0.5 V scanning at 1 V/s. Institutional Review Board approved the collection of clinical samples (Harvard Human Research Protection Program, IRB21-0024).

Detection of antibodies in 96 well ELISA was performed by capturing N protein (100 μL) at concentration of 1 μg/mL for 18 h at 4 °C. Plate was washed and blocked with 5% Blotto (Fisher Scientific, no. NC9544655) for an hour (Najjar et al., 2022). Thereafter, ELISA-plate was incubated with 100 μL of 200-fold diluted plasma samples for half an hour followed by washing and addition of HRP-detection antibody (50 ng/mL). After washing the plate, turbo TMB was pipetted and incubated for 20 min. Following the addition of stop solution, the assay was measured at 450-nm with a plate-reader.

2.3. Screening of detection antibody and capture nucleocapsid (N) protein

For screening of detection antibody, N protein from Raybiotech was immobilized on EC-biosensor and ELISA. For ELISA, 8 positive and 8 negative and for EC-biosensor, 4-positive and 2-negative samples of SARS-CoV-2 were tested. Six screened detection antibodies include anti-Human IgG-HRP (ThermoFisher, no. A18817); Fc-anti-Human IgG−Peroxidase (Millipore Sigma, no. A0170); Peroxidase-F(ab')$_2$ anti-Human-IgG (Jackson-ImmunoResearch, no. 109-036-170); Mouse monoclonal Fc-anti-Human IgG-peroxidase (abcam, no. ab99759); Human Fc-IgG (Bethyl Laboratories, no. A80–148 P); and AffiniPure anti-human Fc-IgG, (Jackson ImmunoResearch, no. 109-005-008). Similarly, for screening of capture N protein 8 positive and 6 negative (ELISA) and 7 positive and 5 negative (EC-biosensor) SARS-CoV-2 samples were tested. 5 different N proteins screened include, N-protein SARS-CoV-2 (GenScript, no. Z03480); Recombinant SARS-CoV-2 N-Protein (RayBiotech, no. 230–30164); SARS-CoV-2 Nucleocapsid (AA 1–419) protein (antibodies-online, no. ABIN6952315); SARS-CoV-2 Nucleocapsid-His recombinant Protein (SinoBiological, no. 40588-V08B); and SARS-CoV-2 Nucleoprotein, His-Tag (NativeAntigen no. REC31851).

2.4. Assay development and optimization

Sandwich ELISA was performed both on EC-sensor and ELISA. Initially, a feasibility study was performed where a biotin-labeled detection antibody followed by the addition of Streptavidin-Poly-HRP (Thermo Fisher, USA) was replaced by HRP labeled detection antibody to reduce the assay steps and complexity. The assay was performed on both ELISA and EC-sensor with 2 positive, 2 negative, and blotto as a negative control. An assay for the optimization of the concentration of detection antibody was then performed on EC-biosensor. 4 positive and 3 negative samples of SARS-CoV-2 were tested with different concentrations of detection antibody ranging from 5 to 80 μg/mL. Likewise, optimization of the concentration of capture N protein from 0.1 to 0.9 μg/mL was performed using 2 positive and 3 negative SARS-CoV-2 samples.

Similarly, the optimum sample dilution study was performed using undiluted and diluted samples (5–15-fold in 1% BSA/rHA) with 3 positive and 2 negative SARS-CoV-2 samples. Finally, optimum assay time was studied where different incubation time of the sample (7–12 min) was performed against TMB incubation time of 1 and 2 min. Furthermore, a titration study was carried out to validate the clinical sample dilution and incubation timing. Three high titer positive samples and two negative samples were taken for the titration study and clinical samples were diluted from 0 to 1000-fold before performing the assay. In addition, a study was performed to compare the effectiveness of rHA over BSA. The assay was performed with 5 positive and 4 negative SARS-CoV-2 samples along with BSA/rHA as a negative control. To overcome the regulatory hurdle of using BSA in a medical device, nanocomposite coating was prepared with BSA and rHA, which was evaluated by performing the whole EC assay. Briefly, the coating was prepared by replacing BSA with rHA followed by functionalization with 0.6 mg/mL N protein or BSA/rHA as negative-control. Then, the sensors were blocked with 15 μL of ethanolamine followed by 10 μL of 2.5% BSA/rHA and the respective buffer was used to run 10-fold diluted SARS-CoV-2 samples (5 positive and 4 negative).

2.5. Anti-SARS-CoV-2 IgG detection on EC-sensor using clinical samples

Optimized assay conditions were used to run clinical samples on EC sensors. 23 positive and 21 negative COVID-19 clinical samples were purchased from Ray Biotech and BWH Crimson Core Laboratory and kept at −80 °C until further use. An additional 23 positive and 14 negative COVID-19 samples were purchased from National Institute for Biological Standards and Control (NIBSC). Similarly, 8 positive and 4 negative COVID-19 Dried Blood Spots on Whatman filter paper #903 were purchased from RayBiotech (CoV-DBS-1) and kept at −80 °C until further use. For reconstitution of DBS, Whatman filter paper with dried blood was kept in a tube and 300 μL of 0.05% PBST was added and kept on a shaker overnight. The reconstituted DBS was then directly used for the assay of anti-SARS-CoV-2-IgG. A time-point study of SARS-CoV-2 was also carried out to understand seroconversion better. Plasma samples were collected on 5 different days (10–21) after the onset of symptoms of COVID-19 for each person. The study was performed with 3 different patients. To run anti-N SARS-CoV-2 Rabbit IgG assay, we immobilized the EC sensor with 0.6 mg/mL N protein or 5 mg/mL rHA as a negative control. After blocking the chip, 15 μL of rabbit SARS-CoV-2-IgG samples were spiked to pre-pandemic plasma samples and incubated on the sensor for half an hour. Then, the sensors were rinsed and 10 μL of 1:1000 Anti-rabbit IgG-HRP (RayBiotech, no. 130-10760-100) prepared in 1% rHA was pipetted to the sensor for 10 min. Sensors were rinsed, and finally, precipitating TMB was pipetted for 1 min before washing and EC measurement. For the calibration curve of NIBSC diagnostic calibrant, the assay was run using the optimized condition in 1% rHA and pre-pandemic plasma sample.

3. Results and discussion

3.1. Single-step assay development

A sandwich ELISA was performed using the EC sensor and an ELISA during assay development. An initial feasibility study was performed where a biotin-labeled detection antibody (followed by washing and addition of streptavidin-polyHRP) was replaced by HRP-labeled detection antibody (single-step assay) to reduce the assay steps and complexity. Using traditional ELISA, with both biotin and HRP-labeled detection antibody, a significantly higher signal for positive samples was observed compared to negative SARS-CoV-2 samples for both the viral N and S proteins (Figs. S1a and b). However, on the EC platform, the HRP-labeled detection antibody showed a higher signal for positive samples and no signal for negative samples as compared to the EC assay with biotin detection antibody where a small signal for 1 negative sample was observed (Figs. S1c and d). Thus, the HRP-linked detection antibody was used for further experiments because it significantly reduces complexity and assay time without compromising assay sensitivity. After the feasibility of the HRP-labeled detection antibody was established, the anti-SARS-CoV-2-IgG detection antibody concentration was varied from 5 to 80 μg/mL to establish a single-step assay (Fig. S2). The concentration-dependent increases in positive signals were observed and 40 μg/mL of detection antibody was determined to be the optimum concentration, which was used in all further experiments.

3.2. Screening of detection antibodies for capture of N protein

Studies have shown that sensitive and specific detection of SARS-CoV-2 antibodies in blood can be obtained by proper choice of capture antigen and detection antibody (human anti-SARS-CoV-2) (Pisanic et al., 2020). We screened 6 commercial SARS-CoV-2-IgG detection antibodies to find the antibody with the highest sensitivity and specificity for the EC platform. Using ELISA, all the detection antibodies showed a similar pattern for positive and negative samples, where up to 25% of positive samples displayed lower signals than one of the negative samples. However, the Sigma and Abcam detection antibodies had comparatively lower signals for negative controls (Fig. S3). When the EC biosensor was used, detection antibodies obtained from Sigma (Fig. 2a), Jackson (Fig. 2b), and Invitrogen (Fig. 2c) could not clearly differentiate between positive and negative samples. However, with Abcam detection antibody, even the low titer positive sample gave a significantly higher signal than negative samples (Fig. 2d). Thus, as the Abcam detection antibody could differentiate all positive and negative samples, it was used for further experiments to obtain a highly sensitive and specific assay.

All viral proteins elicit antibody responses to some extent, but it is necessary to identify proteins to which the immune system best responds and produces the highest affinity antibodies to increase the sensitivity and specificity of a serological assay. Moreover, the more unique the protein is, the lower the cross-reactivity with other coronaviruses (Li and Li, 2020; Petherick, 2020). Thus, we then screened various sources of N protein for their ability to be detected by the Abcam antibody. When tested by ELISA, use of the Genescript N protein resulted in one negative sample showing a similar signal as a positive sample and when N protein from Sinobiological and AIC was used, some positive samples showed lower signals than negative one (Figs. S4b and c). With other N capture proteins, 3 or more positive samples showed lower signals than some negative samples (Fig. S4). When we screened N proteins in the EC biosensor, the N protein from Sinobiological (Fig. 3a), AIC (Fig. 3b), Native Antigen Company (Fig. 3c) produced aberrant signals that did not scale with positive or negative samples. Finally, N capture protein obtained from Raybiotech and Genscript both generated signals for all positive samples, however, the Genscript protein had lower signals in the negative samples (Fig. 3d and e). Thus, Genscript N protein was used for further experiments because it showed high sensitivity and specificity and could differentiate all positive and negative controls.

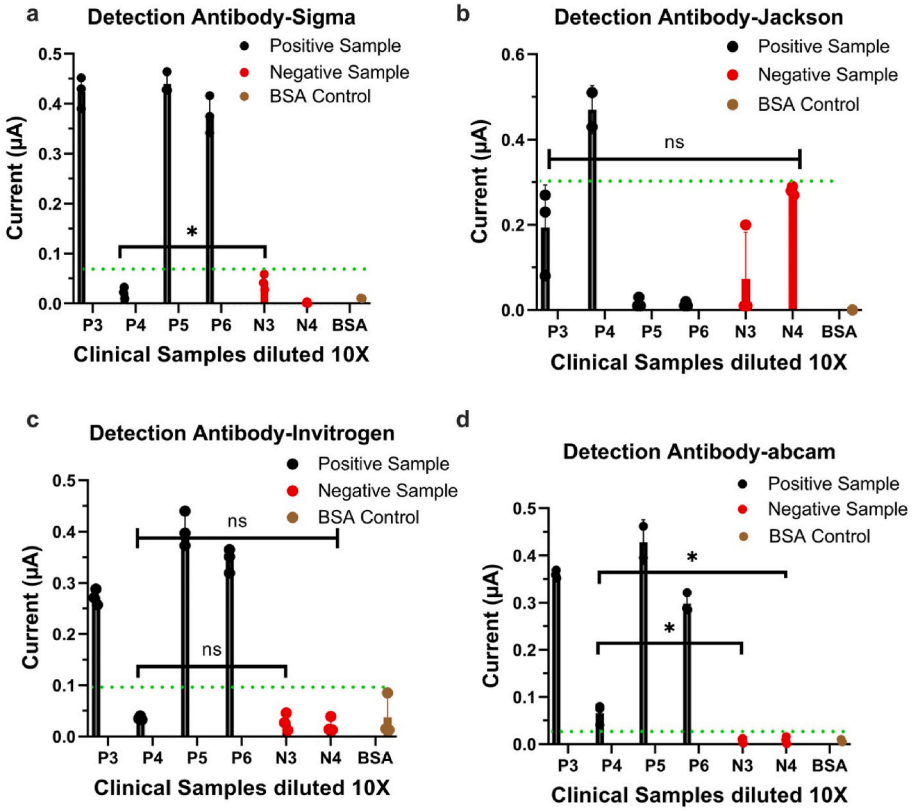

Fig. 2. Screening of anti-human SARS-CoV-2-IgG detection antibody on EC-biosensor from four commercial sources, including Sigma (a), Jackson Immunoresearch (b), Invitrogen (c), and abcam (d). Error bars indicate standard deviation (S.D.) of the mean where n is 3; P= SARS-CoV-2 positive sample; N=SARS-CoV-2 negative sample; and BSA=Negative Control. Green dotted line represents highest signal for negative sample/control. T test (unpaired) was used for statistical analysis ($P > 0.05$ = ns; $P < 0.05$ = *; two tailed).

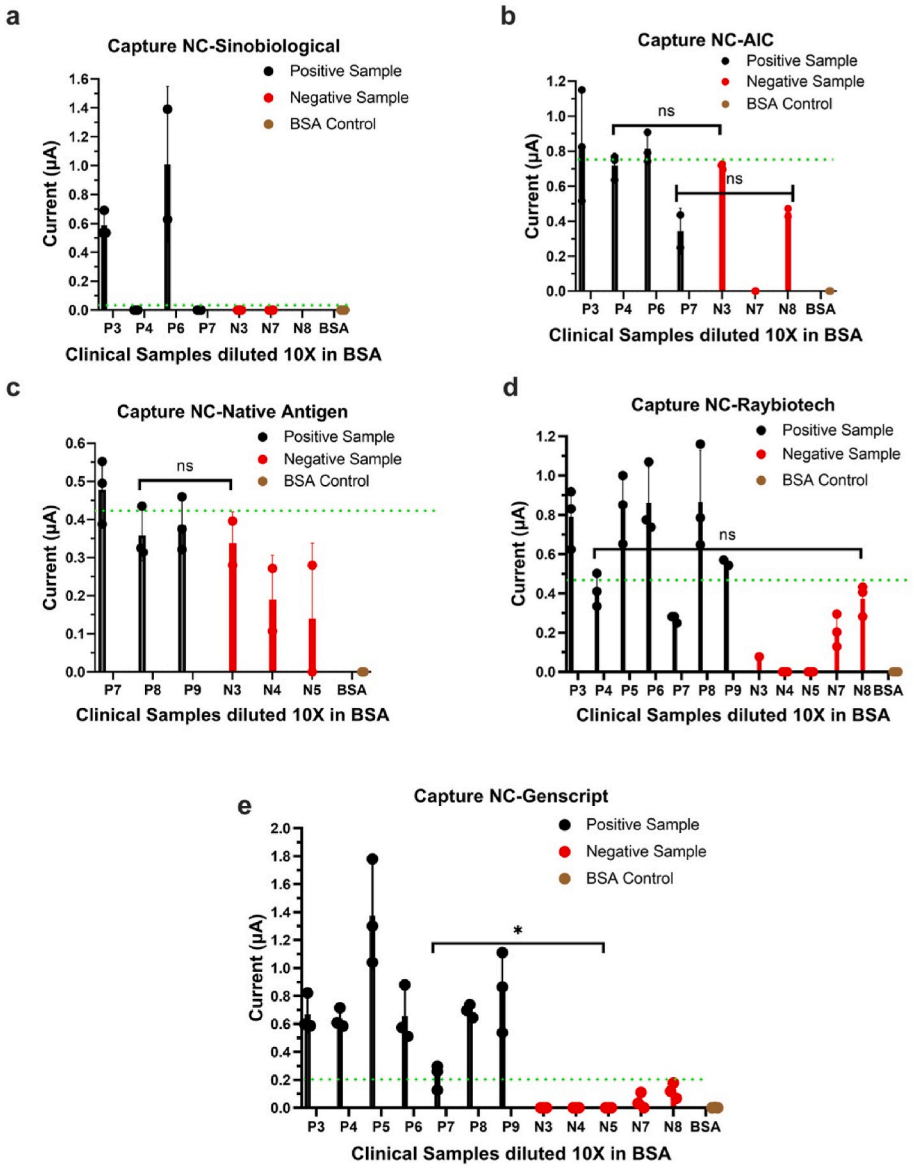

Fig. 3. Screening of SARS-CoV-2 N capture protein on EC-biosensor from five commercial sources, including Sinobiological (a), Advanced Immuno-Chemical (b), Native Antigen Company (c), Raybiotech (d), and Genscript (e). Error bars indicate S.D. where n is 3; P= SARS-CoV-2 positive sample; N=SARS-CoV-2 negative sample; and BSA=Negative Control. Green dotted line represents highest signal for negative sample/control. T test (unpaired) was used for statistical analysis (P > 0.05 = ns; P < 0.05 = *; two tailed). Green dotted line represents signal for negative sample with the highest value.

3.3. Assay optimization

The density of the coated N protein on the surface of the biosensor is key to achieving the surface-to-volume ratio needed for efficient capture and detection of anti-SARS-CoV-2 IgG in the clinical sample. Thus, to reduce non-specific binding and increase assay sensitivity, we examined the effect of varying N protein concentration (from 0.1 to 0.9 μg/mL). These studies revealed the optimum concentration of capture N protein to be 0.6 μg/mL (Fig. 4a).

To avoid the hook and matrix effect, we studied the effect of sample dilution (0–15-fold) to detect anti-SARS-CoV-2-IgG. In general, an increase in signal was observed with positive samples from undiluted to 5- and 10-fold dilution, saturating at 10- to 15-fold (Fig. S5a). Thus 10-fold dilution was considered optimum because below this level of dilution the signal was suppressed, likely due to combined hook and matrix effect.

To better understand the dilution required and the feasibility of rapid testing as a quantitative method, a titration study was performed where samples with high titer of IgG were serially diluted from 0 to 1000-fold (Fig. 4b and Fig. S5b). Signal generated with positive samples increased with 0- to 10-fold dilution, possibly due to the hook's effect. As expected, the negative samples did not show any signal, and the signal for all positive samples decreased proportionally to the increase in dilution from 10- to 1000-fold. Thus, the titration study also revealed that a 10-fold dilution of the sample is optimal for the study.

To perform rapid, sensitive, and specific detection of IgG, we also optimized the sample incubation time and TMB concentration. With 7 min of sample incubation and 1 min of TMB (black bar), all the positive samples showed signals while all negative samples did not (Fig. 4c). When sample incubation time was increased to 8 or 12 min with 1–2 min of TMB, we lost the ability to discriminate between some positive and negative samples. Thus, a sample incubation time of 7 min and TMB precipitation time of 1 min was found to be optimum. In addition, to understand the seroconversion, we performed a time point study using an anti-SARS-CoV-2-IgG clinical sample in three patient groups. As expected, anti-SARS-CoV-2-IgG titers generally increased over the first 17-days after the onset-of-symptoms which is consistent with previous reports (Fig. 4d) (Gilboa et al., 2021).

We also performed an assay to observe if BSA in the antifouling coating and the blocking buffer could be replaced by recombinant human albumin (rHA) without compromising sensitivity and specificity of the assay. We explored rHA as it is blood and animal component-free

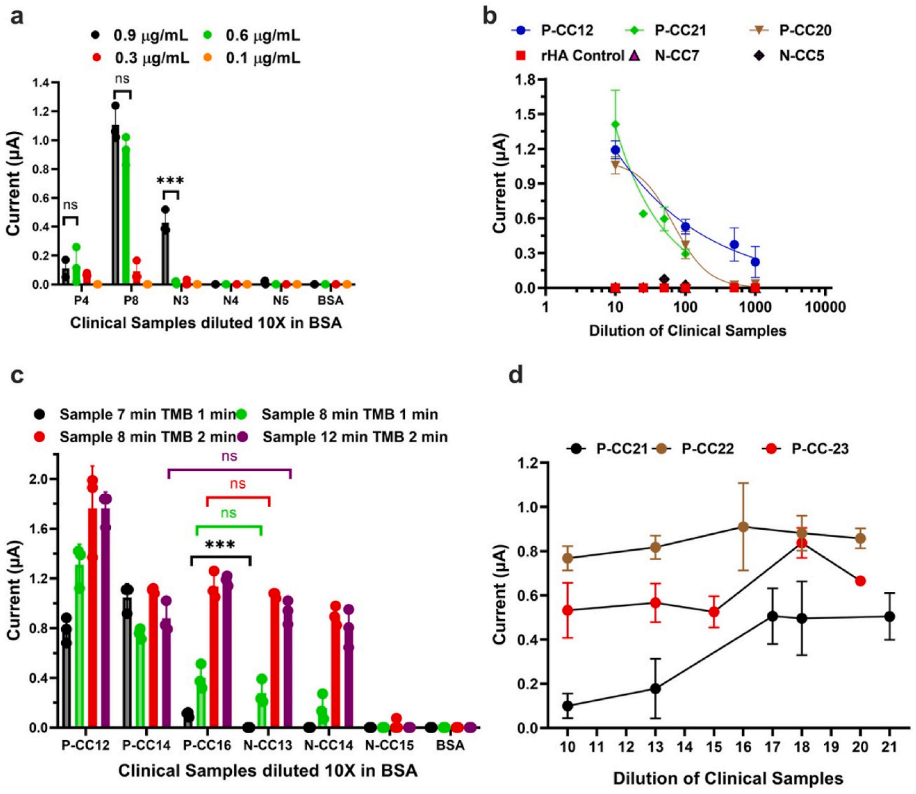

Fig. 4. Assay development and optimization on biosensor. (a) Optimization of concentration of capture N protein. (b) Titration of high titer samples of SARS-CoV-2 on biosensor. (c) Optimization of sample and TMB incubation time for sensitive detection of SARS-CoV-2-IgG. (d) Time-point study of anti-SARS-CoV-2-IgG clinical sample from 10 to 21 days from the onset-of-symptoms. Error bars indicate S.D. where n is 3; P and P-CC= SARS-CoV-2 positive sample; N and N-CC=SARS-CoV-2 negative sample; and BSA=-Negative Control. T test (unpaired) was used for statistical analysis (P > 0.05 = ns; P < 0.001 = ***; two tailed).

recombinant human albumin excipient. rHA is approved by both Food and Drug Administration (FDA, USA) and European Medicines Agency (EMA) (Quinn July 22, 2020). Both BSA and rHA-based coating produced similar signals for all positive samples, however, there was less signal in the negative samples using rHA (Fig. S6).

3.4. Validation of the EC sensor with clinical samples

We then used the EC sensor to test 46 positive and 35 negative SARS-CoV-2 clinical plasma samples to validate its usefulness. These studies revealed that all negative samples showed minimum, or no signal and all the positive samples showed a significantly higher signal (Fig. 5a). Analysis of the ROC curve revealed that the assay displayed 100% sensitivity and 100% specificity with AUC = 1 (Fig. 5b). We then carried out the same assay using 12 DBS samples, which confirmed that the EC sensor can be used to detect IgG in reconstituted dried blood without any further treatment. All positive DBS samples showed signal while none of the negative samples did, which again shows 100% sensitivity and specificity (Fig. 5 c,d). The high sensitivity and specificity of sensor is due to the highly efficient antifouling prGOx/GA/BSA coating, which has very low non-specific binding and allow us to perform the assay in plasma with minimum matrix effect. For a proof-of-concept quantitative assay, the anti-N SARS-CoV-2 rabbit-IgG calibration curve was run using the EC sensor and we detected a sensitivity of 1 ng/mL (Fig. S7a).

The clinical utility of quantitative detection of antibody against SARS-CoV-2 using EC sensor was further validated by generating a calibration curve with anti-SARS-CoV-2 calibrant (NIBSC). Initially, a calibration curve was run with 1% rHA in PBS (Fig. S7b). However, after successful detection of the anti-SARS-CoV-2 diagnostic calibrant in buffer, a pre-pandemic plasma sample without anti-SARS-CoV-2-IgG was used to run the calibration curve, which demonstrated a sensitivity of 0.01 U/mL (Fig. 5e).

4. Conclusion

These results describe the development and validation of an ultra-rapid multiplexed EC-detection platform for monitoring COVID-19 and vaccination status by detecting SARS-CoV-2 antibodies with 100% sensitivity and specificity. The antifouling coating we utilized increases the conductivity of the EC sensor and decreases nonspecific binding, which minimizes the background signals, making the assay more sensitive and selective (Timilsina et al. 2021, 2022b; Najjar et al., 2022). This EC sensor also can be utilized for rapid quantitative detection of SARS-CoV-2-IgG using just 1.5 μL of plasma sample within 10 min with 100% sensitivity and specificity. Thus, through use of the novel antifouling nanocomposite, thorough screening of capture protein and detection antibody, appropriate sample dilution to avoid hook and matrix effect, and rigorous assay development, we were able to develop an ultrasensitive assay with 100% sensitivity and specificity. The potential of the EC-biosensor to perform assay with DBS was also demonstrated using clinical DBS samples with 100% sensitivity and specificity which can be used for serological surveillance utilizing remote sampling and shipment without refrigeration. In addition, validation of the quantitative capability of the EC-sensor was carried out by performing the calibration curve of a NIBSC SARS-CoV-2 calibrant in buffer and pre-pandemic plasma samples. Thus, these studies demonstrate the potential value of this antifouling EC-biosensor which is highly sensitive and selective for rapid quantitative detection of biomarkers in serologic assays and can be carried out in a multiplexed fashion, potentially at the point-of-care (Dou et al., 2017; Wei et al., 2018).

Antibody titers can remain stable for several months and large-scale cohort studies in hospitalized patients show that IgG antibodies against viral proteins correlate with disease severity and outcome. In addition, rapid seroprevalence studies can differentiate reinfections versus breakthrough infections to better understand herd immunity and vaccine efficacy in the context of a pandemic; they also may aid in making important decisions, such as when to reopen economies (DeRoo et al., 2020; Gazit et al., 2021; Gilbert et al., 2021). Hence, this type of

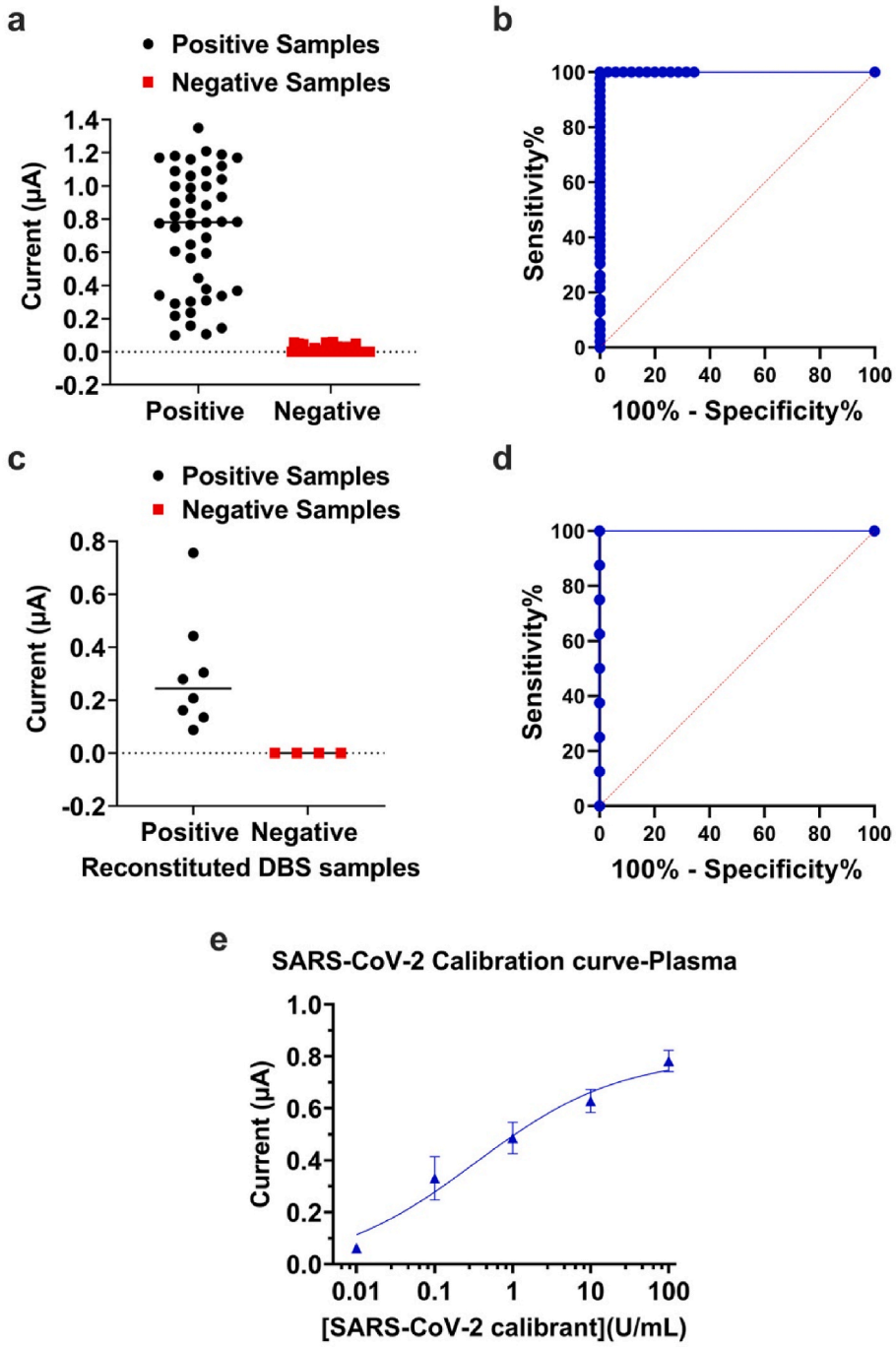

Fig. 5. Clinical validation of the biosensor to detect SARS-CoV-2-IgG. Scattered graph (a) and ROC curve (b) for detection of 46 positive and 35 negative SARS-CoV-2 plasma samples; $P < 0.01$. Scattered graph (c) and ROC curve (d) for detection of 8 positive and 4 negative SARS-CoV-2 clinical Dried Blood Spot; $P < 0.001$. (e) Calibration curve for anti-SARS-CoV-2 calibrant using pre-pandemic plasma sample. Error bars indicate S.D. where n is 6; 4 Parameter-Logistic calibration curve fitting and analysis were carried out.

serological assay could be used to provide a quantitative basis for developing public health strategies and managing responses to COVID-19 as well as other future pandemics. In addition, it helps to understand how patients respond to vaccine and determine if and when boosters are required (Eliakim-Raz et al., 2021; Hamady et al., 2021).

Statistical analysis

All the plate ELISA measurement is presented as the mean of absorbance (a.u.) at 450 nm. Error bars, sample sizes, and statistical tests utilized are defined in the figure legends. Software version 1.1 of Nova was used for analysis and interpretation of data generated using multiplexed sensors. Peak height of the CV generated by TMB was used for the data analysis of biosensors. GraphPad Prism 9 and 4 PL fitting were used for data plotting and statistical analysis.

CRediT authorship contribution statement

Sanjay S. Timilsina: Conceived the study, Ideas were formulated and organized, Experiments were performed and validated. **Nolan Durr:** Experiments were performed and validated. **Pawan Jolly:** Conceived the study, Ideas were formulated and organized, Experiments were performed and validated. **Donald E. Ingber:** Co-conceived the study, Ideas were formulated, Supervised the study, All authors contributed to manuscript preparation and editing.

Declaration of competing interest

This described technology is licensed to StataDX Inc. for neurological, cardiovascular, and kidney disease diagnostics; D.E.I. is a board member and P.J. and D.E.I. hold equity in StataDx; S.S.T., N.D., P.J., and D.E.I are inventors on patents which describes this technology.

Data availability

Data will be made available on request.

Acknowledgments

We gratefully appreciate the research funding from the Wyss Institute for Biologically Inspired Engineering at Harvard University and GBS Inc.

Supporting Information

Supporting Information includes single step assay development, optimization of detection antibody concentration, screening of capture and detection antibody using ELISA, optimization of sample dilution, titration of high titer SARS-CoV-2 positive samples, BSA vs rHA characterization, and calibration curve of SARS-CoV-2 IgG.

Appendix A. Supplementary data

Supplementary data to this article can be found online at https://doi.org/10.1016/j.bios.2022.115037.

References

Abdelhamid, H.N., Badr, G., 2021. Nanotechnol. Environ. Eng. 6 (1), 1–26.
Amini, F., Auma, E., Hsia, Y., Bilton, S., Hall, T., Ramkhelawon, L., Heath, P.T., Le Doare, K., 2021. PLoS One 16 (3), e0248218.
Cabrera, C., Pilobello, K., Dalvin, S., Bobrow, J., Shah, D., Garg, L.F., Chalise, S., Doyle, P., Miller, G.A., Walt, D.R., 2022. Front. Microbiol. 13.
Control; C.f.D., 2017. Prevention Updated October 24, pp. 1–4.
Del Río, J.S., Henry, O.Y., Jolly, P., Ingber, D.E., 2019. Nat. Nanotechnol. 14 (12), 1143–1149.
Demirev, P.A., 2013. Anal. Chem. 85 (2), 779–789.
DeRoo, S.S., Pudalov, N.J., Fu, L.Y., 2020. JAMA 323 (24), 2458–2459.
Dou, M., Sanjay, S.T., Benhabib, M., Xu, F., Li, X., 2015. Talanta 145, 43–54.
Dou, M., Sanjay, S.T., Dominguez, D.C., Liu, P., Xu, F., Li, X., 2017. Biosens. Bioelectron. 87, 865–873.
Eliakim-Raz, N., Leibovici-Weisman, Y., Stemmer, A., Ness, A., Awwad, M., Ghantous, N., Stemmer, S.M., 2021. JAMA 326 (21), 2203–2204.
Elledge, S.K., Zhou, X.X., Byrnes, J.R., Martinko, A.J., Lui, I., Pance, K., Lim, S.A., Glasgow, J.E., Glasgow, A.A., Turcios, K., 2021. Nat. Biotechnol. 1–8.
Flower, B., Brown, J.C., Simmons, B., Moshe, M., Frise, R., Penn, R., Kugathasan, R., Petersen, C., Daunt, A., Ashby, D., 2020. Thorax 75 (12), 1082–1088.
Gazit, S., Shlezinger, R., Perez, G., Lotan, R., Peretz, A., Ben-Tov, A., Cohen, D., Muhsen, K., Chodick, G., Patalon, T., 2021. Clin. Infect. Dis. 75 (1), e545–e551.
Gilbert, P.B., Montefiori, D.C., McDermott, A.B., Fong, Y., Benkeser, D., Deng, W., Zhou, H., Houchens, C.R., Martins, K., Jayashankar, L., 2021. Science, eab3435.
Gilboa, T., Cohen, L., Cheng, C.-A., Lazarovits, R., Uwamanzu-Nna, A., Han, I., Griswold, K., Barry, N., Thompson, D.B., Kohman, R.E., 2021. Angew. Chem. 133 (49), 26170–26176.
Hamady, A., Lee, J., Loboda, Z.A., 2021. Infection 1–15.
Jeyanathan, M., Afkhami, S., Smaill, F., Miller, M.S., Lichty, B.D., Xing, Z., 2020. Nat. Rev. Immunol. 20 (10), 615–632.
Kanjilal, S., Chalise, S., Shah, A.S., Cheng, C.-A., Senussi, Y., Springer, M., Walt, D.R., 2022a. medRxiv. https://doi.org/10.1101/2022.01.10.22269033.
Kanjilal, S., Chalise, S., Shah, A.S., Cheng, C.-A., Senussi, Y., Uddin, R., Thiriveedhi, V., Cho, H.E., Carroll, S., Lemieux, J., Turbett, S., Walt, D.R., 2022b. medRxiv. https://doi.org/10.1101/2022.02.17.22271142.
Kumar, N., Shetti, N.P., Jagannath, S., Aminabhavi, T.M., 2022. Chem. Eng. J. 430, 132966.
Li, D., Li, J., 2020. J. Clin. Microbiol. 59 (5) e02160-02120.
Mavrikou, S., Moschopoulou, G., Tsekouras, V., Kintzios, S., 2020. Sensors 20 (11), 3121.
Michel, M., Bouam, A., Edouard, S., Fenollar, F., Di Pinto, F., Mège, J.-L., Drancourt, M., Vitte, J., 2020. Front. Microbiol. 11.
Morales-Narváez, E., Dincer, C., 2020. Biosens. Bioelectron. 163, 112274.
Najjar, D., Rainbow, J., Sharma Timilsina, S., Jolly, P., De Puig, H., Yafia, M., Durr, N., Sallum, H., Alter, G., Li, J.Z., 2022. Nature Biomed. Eng. 6 (8), 968–978.
Petherick, A., 2020. Lancet 395 (10230), 1101–1102.
Pisanic, N., Randad, P.R., Kruczynski, K., Manabe, Y.C., Thomas, D.L., Pekosz, A., Klein, S.L., Betenbaugh, M.J., Clarke, W.A., Laeyendecker, O., 2020. J. Clin. Microbiol. 59 (1) e02204-02220.
Quinn, K., 2020. IPEC-americas, Webinar. July 22.
Rahman, M.M., 2022. Chemosensors 10 (7), 287.
Rasmi, Y., Li, X., Khan, J., Ozer, T., Choi, J.R., 2021. Anal. Bioanal. Chem. 1–23.
Sanjay, S.T., Dou, M., Sun, J., Li, X., 2016. Sci. Rep. 6 (1), 1–10.
Sanjay, S.T., Fu, G., Dou, M., Xu, F., Liu, R., Qi, H., Li, X., 2015. Analyst 140 (21), 7062–7081.
Sanjay, S.T., Li, M., Zhou, W., Li, X., Li, X., 2020. Microsys. Nanoeng. 6 (1), 1–11.
Seow, J., Graham, C., Merrick, B., Acors, S., Pickering, S., Steel, K.J., Hemmings, O., O'Byrne, A., Kouphou, N., Galao, R.P., 2020. Nature Microbiol. 5 (12), 1598–1607.
Tan, S.S., Saw, S., Chew, K.L., Wang, C., Pajarillaga, A., Khoo, C., Wang, W., Ali, Z.M., Yang, Z., Chan, Y.H., 2021. Arch. Pathol. Lab Med. 145 (1), 32–38.
Timilsina, S.S., Durr, N., Yafia, M., Sallum, H., Jolly, P., Ingber, D.E., 2022a. Advan. Healthcare Mater. 11 (8), 2102244.
Timilsina, S.S., Jolly, P., Durr, N., Yafia, M., Ingber, D.E., 2021. Accounts Chem. Res. 54 (18), 3529–3539.
Timilsina, S.S., Ramasamy, M., Durr, N., Ahmad, R., Jolly, P., Ingber, D.E., 2022b. Advanced Healthcare Materials, 2200589.
Turgeon, C.T., Sanders, K.A., Granger, D., Nett, S.L., Hilgart, H., Matern, D., Theel, E.S., 2021. Diagn. Microbiol. Infect. Dis. 101 (1), 115425.
Wei, X., Zhou, W., Sanjay, S.T., Zhang, J., Jin, Q., Xu, F., Dominguez, D.C., Li, X., 2018. Anal. Chem. 90 (16), 9888–9896.
West, R., Kobokovich, A., Connell, N., Gronvall, G.K., 2021. Trends Microbiol. 29 (3), 214–223.
Wong, M.P., Meas, M.A., Adams, C., Hernandez, S., Green, V., Montoya, M., Hirsch, B.M., Horton, M., Quach, H.L., Quach, D.L., 2022. Microbiol. Spectr. 10 (3) e02471-02421.
Yakoh, A., Pimpitak, U., Rengpipat, S., Hirankarn, N., Chailapakul, O., Chaiyo, S., 2021. Biosens. Bioelectron. 176, 112912.
Zava, T.T., Zava, D.T., 2021. Bioanalysis 13 (1), 13–28.